ChemComm

Accepted Manuscript

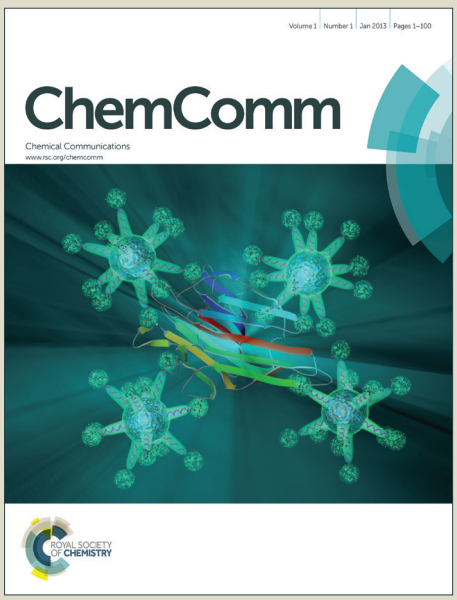

This is an *Accepted Manuscript*, which has been through the Royal Society of Chemistry peer review process and has been accepted for publication.

Accepted Manuscripts are published online shortly after acceptance, before technical editing, formatting and proof reading. Using this free service, authors can make their results available to the community, in citable form, before we publish the edited article. We will replace this *Accepted Manuscript* with the edited and formatted *Advance Article* as soon as it is available.

You can find more information about *Accepted Manuscripts* in the Information for Authors.

Please note that technical editing may introduce minor changes to the text and/or graphics, which may alter content. The journal's standard Terms & Conditions and the Ethical guidelines still apply. In no event shall the Royal Society of Chemistry be held responsible for any errors or omissions in this *Accepted Manuscript* or any consequences arising from the use of any information it contains.

ROYAL SOCIETY OF CHEMISTRY

www.rsc.org/chemcomm

Chemical Communications

RSCPublishing

COMMUNICATION

Self-organized cobalt fluoride nanochannel layers used as a pseudocapacitor material

Cite this: DOI: 10.1039/x0xx00000x

Chong-Yong Lee[a], Zixue Su[a], Kiyoung Lee[a], Hiroaki Tsuchiya[b], Patrik Schmuki[a]*

Received ooth January 2012,
Accepted ooth January 2012

DOI: 10.1039/x0xx00000x

www.rsc.org/

Aligned CoF_2 nanochannel layers have been formed by self-ordering electrochemical anodization. In voltammogramms these layers provide multiple oxidation states, an almost ideal rectangular pseudocapacitive behavior, a high specific capacitance and a good capacitance retention. These layers may thus be promising for supercapacitor applications.

Supercapacitors have matured significantly over the last decade and emerged with the potential to facilitate major advances in energy storage.[1 2] Approaches of the technology can be classified into two categories, namely electrical double layer capacitors (EDLCs) and pseudocapacitors.[3] In contrast to EDLCs, where the charge is stored electrostatically, pseudocapacitors store charge through Faradaic reactions, i.e., they involve the transfer of charge between electrode and electrolyte and thus a red-ox state switching at the electrode materials. In comparison to EDLC, pseudocapacitive materials achieve a substantially higher specific capacitance than EDLC but usually suffer from an inferior rate performance, low utilization yield of active materials, poor cycling stability, and a poor electrical conductivity of the electrode materials.[3] Most common pseudocapacitors are based on suitable transition metal oxides (hydroxides) and conductive polymers.

To enhance the performance of pseudocapacitors, new active materials and construction of pseudocapacitance geometries with large specific surface area, porosity, and suitable electronic conductivity are desired. Hence, nanostructuring efforts target the fabrication of nanoporous morphological structures (e.g., nanotubes,[4 5 6] nanowires[7 8 9]) that exhibit a higher specific capacitance than their bulk material, and also possess a higher stability. Furthermore, one-dimensional nanostructured materials could provide short diffusion lengths to ions and thus lead to higher charge/discharge rates.

Among all the transition metal oxides, hydrous RuO_2 represents the benchmark system with excellent reversibility and ideal solid-state faradaic reactions involving several oxidation states.[10,11] However, the material is relatively expensive for the realization of commercial applications. Spinel cobalt oxides provide a reliable alternative due

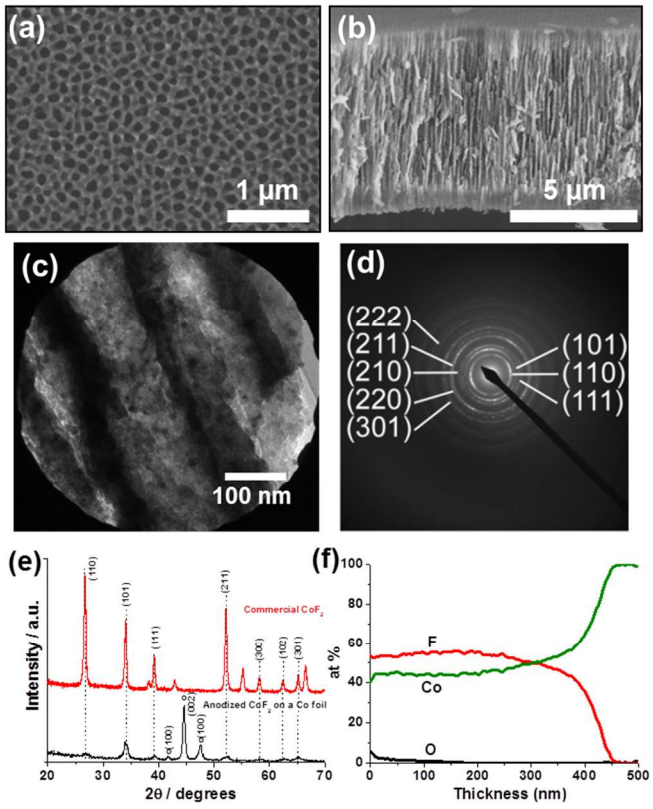

Figure 1 Top (a) and side (b) views of SEM images of the nanoporous anodic CoF_2 layer grown with thickness of 7 µm. c) TEM bright-field image of the anodic CoF_2 nanoporous structure and (d) the corresponding selective area electron diffraction pattern. (e) XRD of the as prepared sample in comparison to the commercially available CoF_2 sample. (f) XPS depth profiles of Co, O, and F of the as anodized CoF_2 sample with a layer thickness of ~ 400nm.

ChemComm Accepted Manuscript

to their low cost and the theoretical high capacitance (3560 Fg^{-1}).[12] Furthermore, several approaches are available to easily form porous surface morphologies and thus to provide the accessibility of electrolyte ions throughout the structure. Recently, we demonstrated that by optimized anodization of Co, a highly aligned nanochannel structure can be formed, which by a suitable heat-treatment can be readily converted to Co_3O_4.[13] These channel layers can be grown up to several 10 micrometers in thickness on the Co substrate with an ordered pore arrangement. In the present work, we show that anodic CoF_2 layers can directly be exploited as pseudocapacitor material with excellent performance. To the best of our knowledge, this is the first demonstration of a fluoride based cobalt compound that exhibits a well-defined two consecutive electron transfer process with excellent pseudocapacitative properties.

The formation of the cobalt fluoride nanoporous layer is, as other cases of self-organizing anodization, based on establishing a suitable formation/dissolution equilibrium.[13-17] We found that anodization in a mixed ethylene glycol and glycerol solvent (volume ratio of 1 to 3) serves the purpose well. Figure 1a shows the top view of a Co sheet after anodizing at 50 V at 0 ^oC for 8 h that leads to an ordered pore structure with pore diameters in the range of 50 to 100 nm (Figure 1a) and a layer thickness of ~ 7 µm (Figure 1b).

Transmission electron microscopy (TEM) images of the CoF_2 structure in Figure 1c show that the nanoporous structures have a wall thickness of ~70 nm. A high degree of crystallinity of CoF_2 is evident from the selected-area electron diffraction (SAED) pattern in Figure 1d. The diffraction patterns can be entirely indexed as CoF_2. The XRD pattern of the layer (Figure 1e) shows a preferential 101 orientation, with peaks that match well with commercially available CoF_2. Figure 1f shows the X-ray photoelectron spectroscopy (XPS) depth profile analyses of the as formed CoF_2 with a layer thickness of ~400nm. As expected, Co and F are dominant in the layer, but an appreciable amount of O is detected that is mainly present in the top layer with a concentration that diminishes across the layer. It can be deduced that the layer is mainly present as CoF_2 that contains a small percentage of cobalt-oxy-fluoride Co-O-F in an amorphous form.

To evaluate the electrochemical properties of the CoF_2 layers, electrochemical measurements were performed in a three-electrode electrochemical configuration with a platinum counter electrode and an Ag/AgCl (3M KCl) reference electrode in 1.0 M KOH solution. SEM examinations of the electrodes after potential cycling (Figure 2a-d) show, in comparison to Figures 1a and 1b, an alteration of the surface morphology. Higher magnification images in Figures 2b and 2d for the top and cross sections show platelet formation on the surface (see also additional SEM images in Figure S1). If Co_3O_4 structures are cycled in KOH solution, the surface morphology remains unaffected as shown in Figure S2. Important to note is however, that although such a surface alteration for the CoF_2 structures upon potential cycling in KOH solution was observed, the nanochannel morphology remains well intact.

The cyclic voltammograms of the CoF_2 and the corresponding Co_3O_4 (converted by thermal annealing in air at 350^oC for 30 min) as shown in Figure 2e reveal the differences in the voltammograms where the latter exhibits a more rectangular shape. Essentially, two distinct redox peaks become apparent for the CoF_2 sample while only one single redox peak in the case of Co_3O_4 is present. This supports that the initial state of the CoF_2 sample is indeed in the oxidation state of two and then undergoes two sequential electron transfer steps from Co(II) to Co(III) and Co(III) to Co(IV). Examination of the scan rate dependence (see Figure S3a) further reveals that the as synthesized CoF_2 possesses faster redox kinetics than Co_3O_4, as shown by the smaller peak to peak separation.

Figure 2f shows the cyclic voltammograms in a narrower potential window of 0 to 0.5 V. The voltammograms exhibit a much more rectangular shape, and essentially the specific areal capacitance can be enhanced by loading a larger amount of CoF_2 via the growth of thicker layers. Note that the gravimetric capacitance calculated from voltammograms at 50 mV s^{-1} exhibit values of 147 ± 5 Fg^{-1} for all layer thicknesses of 0.8, 3.5 and 7 µm. Therefore, no extra capacitance was derived from bulk cobalt foil. The advantage of CoF_2 in comparison to Co_3O_4 is that for the thicker layer, the redox kinetics is still reasonably fast (see supporting information Figure S3a and S3b). This enables the charging/ discharging of a higher amount of material per time and per electrode area. This feature is particularly useful in the case of an application as a microsize capacitor where the areal capacitance becomes important.

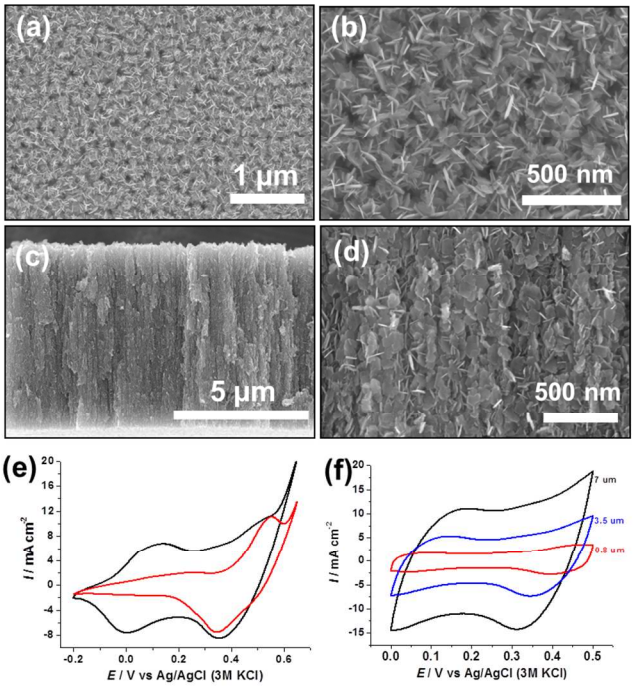

Figure 2 Top (a, b) and cross (c, d) section views of low and high magnification SEM images of the CoF_2 layers after potential cycling in 1M KOH solution. (e) Comparison of the cyclic voltammograms of the CoF_2 layer with Co_3O_4 layer (CoF_2 after heat-treatment at 300^oC for 30 mins) of thickness of 3.5 µm in 1M KOH solution. (f) Cyclic voltammograms of the CoF_2 samples with various layer thicknesses. Scan rate = 50 mVs^{-1}.

Figure 3a shows the cyclic voltammograms as a function of scan rate for a ~7 µm thick CoF_2 layer. The data shows that the voltammograms retain nearly rectangular CV loops up to a scan rate of 100 mVs^{-1}, which are characteristic for supercapacitors with an excellent capacitance behavior and a low contact resistance. Essentially, each curve consists of a capacitive current, and the curves at different scan rates show no peaks; this indicates that the electrodes are charged and discharged at a pseudoconstant rate over the complete voltammetric cycle in this potential range. Variations in the specific capacitance values as a function of scan rates are presented in Figure 3b. At a scan rate of 2 mV/s, a specific capacitance of 268 Fg^{-1} was obtained. The specific capacitance value from this work (204 F g^{-1} at 10 mV s^{-1}) is almost on par with recent work on vertically aligned graphene nanosheets (230 F g^{-1} at 10 mV s^{-1}) – also measured in a three electrode cell configuration.[18] As the

ChemComm Accepted Manuscript

This journal is © The Royal Society of Chemistry 2012

scan rate increases, the specific capacitance of the electrode decreases, as higher scan rate prevents the access of ions to the entire pores of the electrode – the movement of ions is limited by their slow diffusion, and therefore only the outer surface of the electrode can be utilized for charge storage.

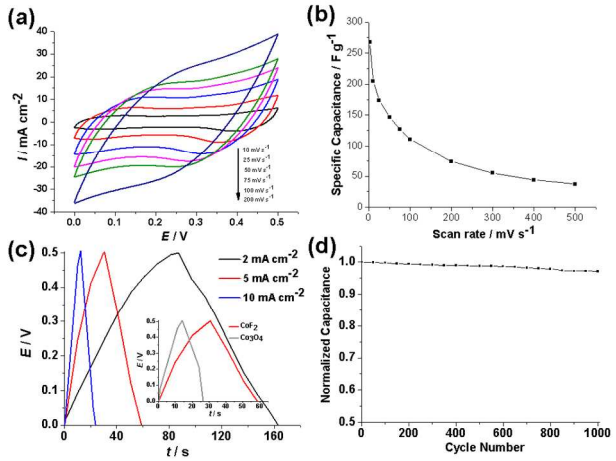

Figure 3 (a) Cyclic voltammograms of a 7 µm thick CoF_2 sample under different scan rates in 1.0 M KOH solution. (b) Plot of specific capacitance vs. scan rate. (c) Galvanostatic charge/discharge curves of the CoF_2 nanoporous layers with different current densities. (d) Capacitance retention test of the CoF_2 nanoporous layers under 1000 CVs cycles at a scan rate of 100 mVs^{-1}.

The galvanostatic charge/discharge curves of CoF_2 collected at various current densities are shown in Figure 3c. The specific capacitance calculated from the curves is 272 Fg^{-1}, 261 Fg^{-1} and 223 Fg^{-1} at a current density of 2, 5 and 10 mA cm^{-2}, respectively. In general, at lower current densities, the specific capacitance decreases with the increase in discharge current density, and the phenomenon is the same as the one observed in the case of increasing scan rate. It should be noted that there is still around 82 % initial capacitance retained (please compare to 272 Fg^{-1} at 2 mA cm^{-2}), even when the current density increases as high as 10 mA cm^{-2}, reflecting the good high-rate performance of the material.

Interestingly, the charge-discharge curves of CoF_2 nanoporous samples are highly symmetric, with only a very slight curvature. This indicates that the supercapacitor behavior is mainly influenced by electrical double-layer contributions (EDLCs) along with the redox reactions (pseudo-capacitors). At 2 mA cm^{-2}, the charge/discharge profile shows only a small IR drop (0.08 V). At 5 mA cm^{-2}, almost a negligible IR drop is seen for CoF_2 samples, however Co_3O_4 samples with the same thickness, as shown in inset of Figure 3c, show a significant IR drop of 0.3 V. This reflects a better electrical conductivity of the CoF_2 samples, with much lower contact resistance. The cycling stability is tested at a scan rate of 100 mV s^{-1} for 1000 continuing voltammetric cycles. One can see that the CoF_2 sample shows a good retention of 97 % of the initial capacitance (Figure 3d). To obtain conclusive information on the layer's long-term stability, significantly extended voltammetric cycling will however be required. Under the present experimental condition, SEM analysis indicates that the aligned channel structure is maintained, although the discussed flake-like morphological changes occur under electrochemical oxidation in KOH electrolyte as presented in Figures 2a-d. Continued voltammetric cycling of a 7 µm thick Co_3O_4 shows an increasing capacitance (see Figure S4) presumably because of better ion transport and penetration to the thick crystalline Co_3O_4 layer for longer cycling.

The enhanced electrochemical capacitive performance of CoF_2 can be attributed to three major factors: Firstly, a faster redox kinetics that facilitates the transport of charge carriers that leads to the higher capacitance. Secondly, the mixed crystalline and amorphous nature of CoF_2 (as shown in the XRD) that increases the density of hydroxyl groups on the cobalt surface, thereby enhancing the pseudocapacitance. Thirdly, the intrinsic properties of CoF_2 with well-defined two-electron transfer process, as multiple oxidation states are beneficial for pseudocapacitor applications.

In summary, we show that aligned CoF_2 channel structure synthesized via anodic growth exhibits excellent supercapacitor properties. The distinct advantage of CoF_2 is that it involves multiple electron transfer from Co(II) to Co(IV) that provides multiple oxidation states with a more rectangular pseudocapacitive behavior, that results in a high specific capacitance and a good performance of high charging/discharging rates. The electrode shows a good capacitance retention from 1000 voltammetric cycles. The present work thus suggests that fluoride based cobalt materials can be considered promising for supercapacitor applications.

Notes and references

This work was supported by grants from the DFG and the DFG cluster of excellence "Engineering of Advanced Materials" (EAM). The authors would like to acknowledge Helga Hildebrand for XPS measurements. A part of the present work was carried out using a facility in the Research Center for Ultra-High Voltage Electron Microscopy, Osaka University.
[a]Department of Materials Science and Engineering, University of Erlangen-Nuremberg, Martensstrasse 7, D-91058 Erlangen, Germany
[b]Division of Materials and Manufacturing Science, Graduate School of Engineering, Osaka University, 2-1 Yamada-oka, Suita, Osaka 565-0871, Japan
*E-mail: (schmuki@ww.uni-erlangen.de)
†Electronic Supplementary Information (ESI) available: Experimental details, SEM images, Cyclic voltammogram. See DOI: 10.1039/c000000x/

[1] J. R. Miller, P. Simon, *Science*, 2008, **321**, 651.
[2] J. Bae, M. K. Song, Y. J. Park, J.M. Kim, M. Liu, Z.L. Wang, *Angew. Chem. Int. Ed.* 2011, **50**, 1683.
[3] B.E. Conway, Electrochemical Supercapacitors: Scientific Fundamentals and Technological Applications; Kluwer: Dordrecht, The Netherlands, 1999.
[4] L. B. Hua, J. W. Choi, Y. Yang, S. Jeong, F. L. Mantia, L. F. Cui, Y. Cui, *Proc. Natl. Acad. Sci. U.S.A.* 2009, **106**, 21490.
[5] G. Wang, Y. Ling, F. Qian, F., X. Yang, X. X. Liu, Y. Li, *J. Power Sources* 2011, **196**, 5209.
[6] M. Kaempgen, C. K. Chan, J. Ma, Y. Cui, G. Gruner, *Nano Lett.* 2009, **9**, 1872.
[7] X. H. Lu, D. Z. Zheng, T. Zhai, Z. Q. Liu, Y. Y. Huang, S. L. Xie, Y. X. Tong, *Energy Environ. Sci.* 2011, **4**, 2915.
[8] H. Xia, J. K. Feng, H. L. Wang, M. O. Lai, L. Lu, *J. Power Sources* 2010, **195**, 4410.
[9] L.-Q Mai, F. Yang, Y.-L. Zhao, X. Xu, L. Xu, Y-Z. Luo, *Nat. Commun.* 2011, **2**, 381.
[10] S. Trasatti, G. Buzzanca, *J. Electroanal. Chem.* 1971, **29** (Appendix 1).
[11] W. Sugimoto, H. Iwata, Y. Yasunaga, Y. Murakami, Y. Takasu, *Angew. Chem. Int. Ed.* 2003, **42**, 4092.
[12] R. B. Rakhi, W. Chen, D. Cha, H. N. Alshareef, *Nano Lett.* 2012, **12**, 2559.
[13] C.-Y. Lee, K. Lee, P. Schmuki, *Angew. Chem. Int. Ed.* 2013, **52**, 2077.
[14] P. Roy, S. Berger, P. Schmuki, *Angew. Chem. Int. Ed.* 2011, **123**, 2956
[15] V. P. Parkhutik, V. I. Shershulsky, *J. Phys. D.* 1992, **25**, 1258.
[16] K. R. Hebert, S. P. Albu, I. Paramasivam, P. Schmuki, *Nat. Mater.*2012, **11**, 162.
[17] Y. Yang, S. P. Albu, D. Kim, P. Schmuki, *Angew. Chem. Int. Ed.* 2011, **50**, 9071.
[18] D. H. Seo, Z. J. Han, S. Kumar, K. Ostrikov, *Adv. Energy Mater.* 2013, **3**, 1316.

ChemComm Accepted Manuscript